



## Chapter 1. Introduction and Overview of Electrogenerated Chemiluminescence

L. Bouffier, N. Sojic

### ► To cite this version:

L. Bouffier, N. Sojic. Chapter 1. Introduction and Overview of Electrogenerated Chemiluminescence. Analytical Electrogenerated Chemiluminescence: From Fundamentals to Bioassays, pp.1-28, 2020, 10.1039/9781788015776-00001 . hal-03084637

**HAL Id: hal-03084637**

**<https://hal.science/hal-03084637>**

Submitted on 26 Nov 2021

**HAL** is a multi-disciplinary open access archive for the deposit and dissemination of scientific research documents, whether they are published or not. The documents may come from teaching and research institutions in France or abroad, or from public or private research centers.

L'archive ouverte pluridisciplinaire **HAL**, est destinée au dépôt et à la diffusion de documents scientifiques de niveau recherche, publiés ou non, émanant des établissements d'enseignement et de recherche français ou étrangers, des laboratoires publics ou privés.

## CHAPTER 1

### Introduction and overview of electrogenerated chemiluminescence

L. Bouffier, N. Sojic

University of Bordeaux, Bordeaux INP, ISM, UMR CNRS 5255, 33607 Pessac, France

\*Corresponding contributor. E-mail: [Neso.Sojic@enscbp.fr](mailto:Neso.Sojic@enscbp.fr)

#### Abstract

This chapter is conceived as a general introduction to electrogenerated chemiluminescence (ECL) for those without prior knowledge of the subject, but with a background in chemistry or biochemistry. The major processes, methods and concepts discussed in this chapter give only a foundation for a first understanding of ECL. After a simple classification of the different types of luminescence, we present the underlying principles of ECL in electrochemistry and photophysics. The basic energetic and kinetic aspects, which involve exergonic electron-transfer reactions are then introduced and briefly described by the Marcus theory. We consider then the different mechanistic pathways leading to the generation of the electronically excited state of the luminophore. This is followed by a short presentation of the main protagonists: the electrode materials, where ECL is initiated, the nature of the luminophores and of the coreactants. Finally, the sensing strategies are presented with the main (bio)analytical applications, which are nowadays successfully commercialized.

## 1. Introduction

Electrogenerated chemiluminescence, also called electrochemiluminescence (ECL), is the production of light by an excited luminophore species (an atom, a molecular entity or a nanoparticle) generated during an electrochemical reaction.<sup>1-7</sup> It means that ECL begins always with an electron-transfer reaction at the electrode surface. This initial electrochemical step triggers a cascade of chemical reactions of reactive intermediates that undergo highly exergonic homogeneous electron-transfer reactions to generate finally the electronically excited state of the luminophore (or electrochemiluminophore). It relaxes to the ground state by emitting a photon. In brief, as the word implies, ECL is initiated by an electrochemical triggering reaction (“E”), continues with a homogeneous chemical step (“C”), which leads *in fine* to the formation of the excited state, and ends with a luminescent step (i.e. light emission, “L”).

ECL belongs to the family of luminescence processes. The word luminescence comes from the Latin “*lumen*”, which means light. It was first introduced as “*luminescenz*” by the physicist E. Wiedemann in 1888 to describe “*all those phenomena of light which are not solely conditioned by the rise in temperature*”, as opposed to incandescence.<sup>8</sup> Luminescence corresponds to cold light whereas incandescence is hot light. Luminescence processes can be classified according to the nature of the reaction providing the energy to reach the excited state of the luminophore.

[Table 1 near here]

Table 1 shows some representative phenomena, which are capable of showing light emission. Typically, for photoluminescence phenomena, such as fluorescence or phosphorescence, the energy source is the photon absorbed by the luminophore (i.e. photo-excitation). In chemiluminescence (CL), the energy is provided by the homogeneous chemical reaction(s) between at least two reagents (i.e. chemi-excitation). ECL is a specific case where these reactive species are produced electrochemically at the electrode surface (i.e. electro-chemi-excitation).

Even if the same chemical system may generate diverse types of luminescence, it is important to distinguish ECL from CL as well as from electroluminescence. On one hand, CL is produced in the bulk by mixing the reactive species and is controlled by the fluid flow. On the other hand, ECL is initiated by applying the electrode potential and the reagents are produced *in situ* electrochemically. Their reaction leads to ECL emission in the immediate vicinity of the electrode surface (controlled by diffusion) and not in the bulk as in CL. Furthermore, electroluminescence is the radiative recombination of electrons and holes in a material, usually a semiconductor. Therefore, ECL differs from electroluminescence by the nature of the reactions generating the excited state. In brief, CL, ECL and electroluminescence are all light-emitting phenomena that do not require an optical excitation.

The first observations of light emission during electrolysis were published using Grignard compounds and luminol (5-amino-2,3-dihydro-1,4-phthalazinedione) in the 1920s.<sup>9, 10</sup> They reported irreversible ECL systems involving bond-breaking reactions (*vide infra*) within the luminophore structures (e.g. luminol). This type of ECL can also be considered as atom-transfer reaction and it provides enough energy to populate the excited state. However, a revolution in the ECL field started in the mid-1960s, more precisely with reports published during the summer/autumn 1964<sup>11-14</sup> on electron-transfer excitation reactions (*vide infra*). Indeed, the first detailed investigations of such reversible ECL systems involving radical ion annihilation reactions were then described by several groups.<sup>12-14</sup> From a historical point of view, the roots of this research are found in the electrochemical generation of aromatic hydrocarbon radical ions, because the dominant dogma promoted in organic chemistry at that time was that the electrons go by pairs and not one by one, as largely demonstrated since then.<sup>4</sup> Hercules reported first the “*production of chemiluminescence during electrolysis of aromatic hydrocarbons*”.<sup>12</sup> He obtained “*electrochemically generated luminescence*” from several hydrocarbons such as anthracene, pyrene, rubrene in N,N-dimethylformamide (DMF) or acetonitrile solvents by

using two main configurations: 1) by alternating the current or 2) by applying a current at two closely spaced electrodes.<sup>12</sup> This sharp seminal report contains remarkable original ideas and suggestions on the stability of the electrogenerated species, the possible mechanisms, the experimental configurations, ECL imaging as illustrated by the ECL photograph of the concentric electrode grids, etc. This work was published almost simultaneously with another article on CL electron-transfer reactions obtained by recombination (i.e. annihilation) between anion and cation radicals of 9,10-diphenylanthracene (DPA) that were prepared chemically.<sup>11</sup> A few months later, the same group published annihilation ECL of electrogenerated DPA radicals.<sup>13</sup> This example shows how ECL and CL histories are intrinsically related, as also illustrated by other examples in the following decades.<sup>11, 15-22</sup> Indeed, CL and ECL processes are similar in nature; they share some common features and theoretical fundamentals (Chapter 2).<sup>23, 24</sup> It is interesting to notice that E. A. Chandross mentioned that “*a chemiluminescent reaction between electro-generated anthracene positive and negative radical ions has been observed by Hoijtink and co-workers*” (private communication during a visit in the summer of 1963).<sup>11</sup> However, these results were never published by G. J. Hoijtink. The groups of Chandross and Bard used cyclic voltammetry to study the anodic and cathodic processes of these aromatic hydrocarbons and thus to clarify the annihilation mechanism leading to ECL emission.<sup>13, 14</sup> These initial works have been rapidly followed by many other practical and theoretical developments. Some of the key-milestones in this context are depicted in Scheme 1, which is certainly a very subjective and non-exhaustive list of examples.

[Scheme 1 near here]

For instance,  $[\text{Ru}(\text{bpy})_3]^{2+}$  is a model ECL luminophore that is largely used even nowadays and Tokel and Bard reported in the 1970s the first example of ECL derived from electrogenerated species of the  $[\text{Ru}(\text{bpy})_3]^{2+}$  complex.<sup>16</sup> ECL as well as CL resulting from simple electron-transfer reactions have been treated theoretically by R. A. Marcus.<sup>23-25</sup> The discovery of ECL

emission in aqueous media<sup>26</sup> with efficient coreactants (Chapter 4) such as tri-*n*-propylamine (TPrA)<sup>22</sup> has led to successfully commercialized bioassays for clinical diagnostics (Chapter 15).<sup>27, 28</sup> The early ECL studies were based on ion annihilation and this fundamental research was essential to pave the way for coreactant ECL, which is almost exclusively used nowadays for (bio)analytical applications.

## **2. Fundamentals of electrochemistry and photophysics for ECL**

As already mentioned, the first step in all ECL processes is an electron-transfer reaction occurring at the electrode surface whereas the final step is the light emission that involves transitions between electronic states of the luminophore. Therefore, reactions involving electrons are at the core of the ECL phenomenon and ECL intimately combines concepts and methods from electrochemistry and photochemistry. Moreover, the electronic states and in particular the frontier orbitals of the luminophore govern its electrochemical and photophysical properties and thus the resulting ECL behavior. Electrochemical techniques of characterizing redox properties of the luminophore (and of the coreactant) often complement the spectroscopic techniques. Both approaches are essential to investigate in details an ECL system.

### **2.1. Basic electrochemical principles**

The heterogeneous electron-transfer reaction between an electrode surface and the redox species dissolved in the electrolyte solution is the fundamental process in electrochemistry.<sup>1</sup> On the one hand, the potential of an electrode is an expression of the energy of the electrons in the electrode (i.e. Fermi level).<sup>1</sup> By changing the electrode potential with a potentiostat, the electron energy within the electrode is tuned continuously over a wide range. On the other hand, for the dissolved species, the frontier molecular orbitals such as the HOMO (highest occupied

molecular orbital) and LUMO (lowest unoccupied molecular orbital) define the electrochemical reactivity for simple redox processes. Therefore, by imposing progressively more negative potentials, the electron energy of the electrode is raised and an electron can be transferred from the electrode into the vacant electronic state (i.e. LUMO) of the chemical species. This reaction is called reduction (Figure 1a). By contrast, by driving the potentials to more positive values, the electron energy of the electrode decreases and an electron can be transferred from the chemical species into the electrode. Since the HOMO is the orbital of highest energy that is occupied, an electron is removed from this orbital and it is therefore an oxidation reaction (Figure 1b). In a first order approximation, the electrochemical potentials found for reduction and oxidation reactions provide data on the HOMO and LUMO energies of the considered species.

[Figure 1 near here]

Depending on the applied potential  $E$ , each species that is either reduced or oxidized accepts or gives up an electron from/to the working electrode, respectively. Since electrons cross the electrode|solution interface, the current  $i$  flows in the circuit between the working electrode and the counter-electrode. The measured current (i.e. flow of electrons across the electrode) is directly proportional to the reaction rate of the electrochemical reaction taking place at the electrode, so to the number of transformed species.

To examine the electrochemical properties of a redox species, the electron energy within the electrode is tuned continuously by sweeping linearly the potential of the working electrode over a wide range. In such a typical experiments called cyclic voltammetry, the potential is swept with time starting from a potential where no electrochemical reaction occurs and moving to potentials where reduction or oxidation of the redox species takes place. After passing the potential at which redox reactions can occur, the direction of the linear sweep is reversed and

the species electrogenerated during the forward scan may be detected during the backward scan, depending on their stability. The most common format for presenting electrochemical data is a plot of current as a function of the electrode potential ( $i$  vs.  $E$ ). This  $i$  vs.  $E$  curve can be considered as the electrochemical equivalent of a spectrum obtained in spectroscopy.<sup>29</sup> Indeed, in absorption and emission spectra, the properties of the dye and the electronic transitions are probed by scanning its responses for incident photons with different energies. In a cyclic voltammogram, the redox properties of the dissolved species are investigated by tuning the energy of the electrons in the electrode (i.e. by scanning the electrode potential). Figure 2 shows a cyclic voltammogram of a rubrene solution containing a supporting electrolyte. Reversible oxidation waves forming the cation radical and reduction forming the anion radical are clearly visible.

[Figure 2 near here]

The time scale of such voltammetric experiments is controlled by the scan rate of the potential. Several important parameters characterize the recorded signal: the cathodic and anodic peak potentials, the cathodic and anodic peak currents, the half-peak potential and the half-wave potential. In the case of ECL, light intensity is also measured during such experiments and current as well as ECL intensity are plotted vs. potential ( $i$  and  $ECL$  vs.  $E$ ). The curves are very informative about the thermodynamic and the kinetics of the reactions that occur at the interface, the stability of the species upon electron-transfer, and more generally about the reactivity of the electrogenerated species. They provide very valuable information to study and to decipher the different ECL mechanistic pathways (Chapter 5).

## 2.2. Basic photophysical principles



Luminescence (e.g. fluorescence, phosphorescence, CL, ECL, *etc.*) is the radiative process that involves transition between electronic states of the luminophores. In the ground state, the electrons fill progressively the various atomic orbitals with the lowest energies in pairs. Pauli exclusion principle dictates that two electrons in one given orbital must have spins in opposite directions and then the total spin is equal to 0. Since the fundamental electronic state of a given luminophore A presents in general no net electron spin, its spin multiplicity ( $2S + 1$ ) is equal to 1 and, for this reason, this ground state is named singlet and noted  $S_0$  or  $^1A$ . Absorption of a photon with the adequate quanta energy provokes the excitation of the luminophore due to the promotion of one electron from the highest occupied orbital to a previously unoccupied orbital having a higher energy. Typically, the energetically-lowest electronic transition occurs between the HOMO and the LUMO (Figure 3a). The energy difference between these two frontier orbitals is termed the HOMO–LUMO gap. Figure 3b shows a diagram, known as the Jablonski diagram, which is very convenient to visualize the photophysical processes and their respective kinetics or lifetimes. It shows the two electronically excited states with the lowest energy: the singlet ( $S_1$ ) and the triplet ( $T_1$ ). The terms singlet and triplet refer to the spin multiplicity of an electronic state.

[Figure 3 near here]

Absorption is a very fast event ( $\approx 10^{-15}$  s) in comparison to the other processes so that during this step, there is no displacement of the nuclei according to the Franck–Condon principle. It means that, in the first instant after the generation of the electronically excited state, the luminophore is just like in the fundamental state as far as positions and kinetic energies are considered, but with a very different electronic configuration. At equilibrium, molecules have the greatest probability of having the thermal energy of the lowest vibrational levels of the ground state in accordance with the Boltzmann distribution. The vertical arrows (blue lines) correspond to the absorption process, which starts from the lowest vibrational energy level of

the fundamental electronic state  $S_0$  to reach one of the vibrational levels of the electronic excited state  $S_1$ . Then it deactivates very rapidly ( $\approx 10^{-13}$  -  $10^{-11}$  s) to the lower vibronic levels of  $S_1$ . This vibrational relaxation (red arrows) is faster than the electronic transition and the corresponding vibrational excess energy dissipates as thermal energy to the surrounding medium, typically to the solvent molecules. Indeed, it should be noted that the luminophores remain in the excited singlet state for a given period of time, from a few tens of picoseconds to a few hundred nanoseconds, depending on their structure, the medium and the experimental conditions. From  $S_1$ , the luminophore may follow several competitive de-excitation pathways:

- emit a photon during the electronic transition  $S_1 \rightarrow S_0$ . This radiative process is called fluorescence (Figure 3b). The difference between the absorption and emission band maxima is known as the Stokes shift.
- relax to the fundamental state  $S_0$  without photon emission by internal conversion. This process is defined as a non-radiative transition between two electronic states of the same spin multiplicity (spin conservation rule).
- undergo a non-radiative transition between two isoenergetic vibronic levels from electronic states of different spin multiplicities. It requires a spin flip of one of the unpaired electrons. This process named intersystem crossing ( $\approx 10^{-9}$  s) occurs from  $S_1$  to  $T_1$  in the present simplified example (horizontal green arrow). It competes with the fluorescence  $S_1 \rightarrow S_0$  path. Such a transition is in principle forbidden but the effects of the spin-orbit coupling (i.e. coupling between the orbital magnetic moment and the spin magnetic moment) can be strong enough to make it possible. This coupling can be enhanced by the presence of heavy atoms (i.e. with nuclei of high electronic density).
- deactivate in a non-radiative fashion to the ground state by either energy-transfer or electron-transfer with another molecule called a quencher. This path is not presented on

Figure 3b for sake of clarity. A common example of a molecule that quenches many excited singlet (and triplet) states is dioxygen whose ground state is a triplet.

If intersystem crossing from  $S_1$  to  $T_1$  occurs, the luminophore transits via the triplet state. From  $T_1$ , the luminophore may deactivate to the ground state  $S_0$  by emitting a photon. This phenomenon is called phosphorescence (Figure 3b). It competes with the intersystem crossing (from  $T_1$  to  $S_0$ ), which is a non-radiative process. In solution at room temperature, this non-radiative relaxation  $T_1 \rightarrow S_0$  is predominant over phosphorescence. Another alternative is the triplet-triplet annihilation that leads to the singlet state (vide infra). In addition, the phosphorescence band is shifted to higher wavelengths than the fluorescence one, because  $T_1$  is lower in energy than  $S_1$ .

The formula  $E = h\nu$  allows to relate the position of the observed spectral band maximum ( $\lambda$ ) to the energy difference between the initial and final states involved in the electronic transition. Therefore, the energy  $E_s$  required to produce the lowest excited singlet state from the ground state can be estimated, in a first order approximation, using the relation:

$$E_s(\text{in eV}) = \frac{hc}{\lambda} = \frac{1239.8}{\lambda(\text{in nm})} \quad (1)$$

The comparison between the recorded ECL and photoluminescence (fluorescence or phosphorescence) spectra may indicate whether the same emissive state is reached by both excitation modes.

### 2.3. Energetics and kinetics

Light emission according to ECL does result from an intimate interplay between electrochemistry and photochemistry. The excited state of the luminophore is populated by a

sequence of events that is initiated by a first electrochemical step. However, the ECL phenomenon is only possible under specific circumstances that are enabled through thermodynamics and kinetics control. ECL mechanisms have been extensively studied in the past and can take place according to many different pathways (cf. section 3). But the starting point is invariably an electron-transfer step. Typically, a redox-active molecule that could be either the luminophore or a coreactant undergoes an oxidation or a reduction at the electrode surface. This heterogeneous electrochemical step is then followed by a series of chemical steps that allows the simultaneous presence of highly reactive species at the vicinity of the electrode (i.e. reaction layer). From a thermodynamics point of view, it is clear that the co-existence of these species is unlikely and they are therefore involved in a very energetically favourable reaction (typically, an atom-transfer decomposition and/or a redox reaction).

From a thermodynamic point of view, the possibility to produce light according to a given ECL process is governed by the free-enthalpy of the corresponding redox reaction that yield back the luminophore and/or decomposition products. Indeed, this free-enthalpy is directly given by the difference of potentials of the involved reactive redox species according to:

$$\Delta G^{\circ}(\text{in eV}) = E^{\circ}_{(Ox1/Red1)} - E^{\circ}_{(Ox2/Red2)} \quad (2)$$

Here, this equation is written regardless the nature of the redox species with the first potential corresponding to the species generated by reduction and the second one by oxidation according to sign convention. The standard potentials of the redox couples are typically extracted from a cyclic voltammetry experiment recorded by using a solution of the ECL precursors in case of an annihilation reaction and/or inferred from more sophisticated experiments or calculations when a coreactant is involved.<sup>30</sup> The  $\Delta G^{\circ}$  value can be compared to the energy  $E_S$  of the emitted photons in order to define if the ECL system investigated is energy-sufficient or not. The difference between  $\Delta G^{\circ}$  and  $E_S$  is also a reasonable indicator of the ECL efficiency when

comparing a series of dyes that undergo a comparable ECL mechanism and that present similar quantum yields. Yet, this simple thermodynamic comparison does not take into account special mechanisms (see T-route discussed in the next section) or for example the formation of excimers, etc.

Several authors proposed to visualize such thermodynamic (or energetic) requirements in a simple graphic that displays electrochemical *versus* photoluminescence data.<sup>31, 32</sup> This representation called “ECL wall of energy sufficiency” was reported first by Hogan and co-workers with a series of iridium-based inorganic complexes.<sup>31</sup> In all cases, an ECL luminophore is positioned on the graphic according to two coordinates, one being a function of the redox potential and the other depending on the emission wavelength. Also, a mathematical curve corresponding to the equation  $\Delta G^\circ = E_S$  does split the graphic into two zones where ECL is either enabled (in white) or forbidden (in grey), respectively. The characterization of a series of iridium complexes labelled from 1 to 5, as well as two reference inorganic dyes is gathered in Figure 4. This formalism offers a straightforward way to schematize the ECL threshold and compare qualitatively the ECL efficiency between dyes that are ECL active or not.

[Figure 4 near here]

The ECL yield is not straightforward to estimate. It depends indeed of the luminophore and eventually the coreactant employed because the experimental conditions (solvent, concentration, applied potential, electrode material, etc.) will determine the predominant ECL mechanism. The intensity of the emitted light is linked with the efficiency of generating the excited state that depends on the rate of the annihilation reaction.<sup>33</sup> During the process, the redox state of the luminophore is changed either by an electrochemical (i.e. heterogeneous reaction at the electrode|solution interface) or a redox (homogeneous reaction in solution) mean. Here, there is also a competition between the formation of the luminophore in the excited state

or ground state (see below). Finally, the amount of dye that reached the excited state can return to the ground state by radiative or non-radiative emission, meaning that the quantum yield of the luminophore is also involved in the calculation of the ECL yield. In photoluminescence, relative quantum yields can be determined by comparing the fluorescence strength between a given substance and a reference luminophore of known quantum yield for the same experimental parameters (excitation wavelength, excitation and emission slit widths, photomultiplier voltage, etc.). The ECL yield is estimated in a comparable manner by using most of the time  $[\text{Ru}(\text{bpy})_3]^{2+}$  as a reference compound. Somehow, the overall yield can be deconvoluted into two contributions: the efficiencies to produce the excited state and to emit light from this state, respectively. Therefore, an intrinsically low ECL yield might be solely limited by one of these parameters but not necessarily both.

Again, ECL is a particular case of CL where the process is initiated by electrochemistry. An efficient light production necessitates fulfilling a number of criteria such as the involvement of suitable chemical species to populate the excited state. A key parameter is the compromise between the choice of the emitter in relation to the thermodynamic of the process (sufficient excitation energy, rapid reaction rate, competition between the formation of excited state *versus* ground state, etc.). The chemical nature of the luminophore does determine the energy requisite through a direct relationship between the emitted wavelength of light and the energetic threshold. Considering equation 1, this typically ranges between 2.07 eV for red light ( $\lambda = 600$  nm), 2.48 eV for green light ( $\lambda = 500$  nm) and 2.75 eV for blue light ( $\lambda = 450$  nm), respectively. The involved reactions are indeed very energetic (2-3 eV) and extremely fast (up to molecular vibration timescale), leading to an unexpected manifestation of the Franck-Condon principle. In fact, during this electron-transfer step, the involved molecules cannot easily accommodate such a large amount of energy on a short timescale. This is why the formation of the excited state is favored compared to the ground state in order to minimize the mechanical constraint

(i.e. rotational, vibrational and/or translational modes). Another way to understand this kinetic manifestation is to consider the ECL phenomenon within the theoretical framework of electron-transfer developed by R. A. Marcus in the mid 60's (Chapter 2).<sup>23-25</sup> In this formalism, the potential surfaces are graphically represented with the  $x$  axis being the reaction coordinate (reflecting changes in nuclei position) and the  $y$  axis being the energy (Figure 5a). The reactant state is on the left and the chemical pathway through a hill reaches the product state on the right. As a reminder, the rate constant  $k$  of the process is proportional to  $e^{-E_a/k_B T}$ , with  $E_a$  being the activation energy (Figure 5). Mathematically, these potential energy curves can be described as parabolas taking into account the simple model where atoms are connected by a spring. In this case, the energy depends on the square of the distance between nuclei. The theory of Marcus provided the following very simple expression between the activation energy  $E_a$ , the Gibbs energy  $\Delta G^\circ$  and the reorganization energy  $\lambda$ :  $E_a = \frac{(\Delta G^\circ + \lambda)^2}{4\lambda}$ . One of the corollary of this formalism is the distinction between two regions when drawing the kinetics ( $\ln k$ ) as a function of the thermodynamics ( $-\Delta G^\circ$ ) of the process (Figure 5c). The normal region reflects the increase of the reaction rate with free enthalpy. In contrast, the inverted region reflects the kinetic inhibition occurring with particularly exergonic reactions. Indeed, this is the relevant situation in the case of ECL where the thermodynamic product (i.e. ground state) is kinetically inhibited in favor of the excited state.

[Figure 5 near here]

### 3. Mechanistic pathways of ECL

ECL is initiated by a heterogeneous triggering electron-transfer reaction at the electrode surface. It can be produced through several principal pathways. Scheme 2 shows the dominant branches with the subsequent sub-pathways. We classified them according to the nature of the final reaction producing the emissive state of the luminophore. After the first triggering

electrochemical step at the electrode surface, this excitation reaction involves either homogeneous electron-transfer reactions implying the luminophore, bond-breaking reactions within the luminophore frames or a special route called hot electron-induced ECL. The main difference between the first two pathways is the regeneration of the luminophore in the first case whereas it is not the case for the second one because it involves an irreversible ECL system with bond-breaking or atom-transfer reaction. In other words, in the path named bond-breaking reactions of the luminophore, the luminophore can emit a photon just once during the process because it involves an irreversible step. In the case of the electron-transfer reaction, the luminophore is regenerated at the end of the ECL mechanism. Therefore, it can be reused and it produces numerous photons during the ECL process.

[Scheme 2 near here]

### **3.1. Electron-transfer reactions involving the luminophore**

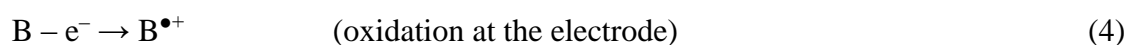
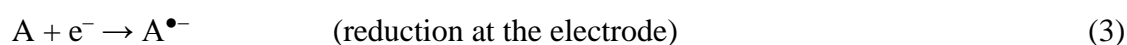
For this path, the emissive state of the luminophore is produced by an exergonic electron-transfer reaction occurring in solution and involving directly the luminophore. Two species (or two redox states of the same species) undergo a homogeneous electron-transfer reaction to produce the excited state. Since the electron-transfer reaction is a reversible process when not associated to a chemical step, the luminophore is regenerated at the end of the ECL mechanism. One can distinguish two main sub-pathways through which ECL is promoted, namely the annihilation and coreactant pathways (Chapter 5).

#### **3.1.1. Annihilation pathway**

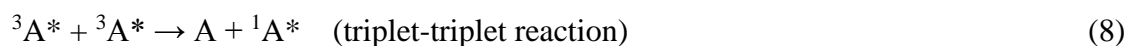
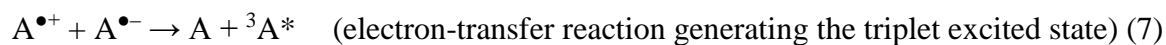
In the annihilation pathway, reduced  $A^{\bullet-}$  and oxidized  $B^{\bullet+}$  species are electrochemically produced (respectively, reactions 3-4) either at two different electrodes positioned closed



enough or at the same electrode surface by applying alternating pulsed potentials. Then these two intermediates diffuse and recombine according to an ion annihilation reaction, also called comproportionation reaction. This homogeneous electron-transfer reaction between  $A^{\bullet-}$  and  $B^{\bullet+}$  (reaction 5) generates the electronically excited state  $^1A^*$  of the luminophore (Figure 6). It is important to notice that A and B can be the same initial molecule, and then just the redox states are different.



If the annihilation reaction is exergonic enough, it populates directly the emitting singlet excited state of the luminophore. In this case, the free energy of the reaction is greater than or equal to the energy of the emissive singlet state  $E_S$  and the emitted ECL follows the singlet route, also called “S-route” (Scheme 2). However, if the energy of the annihilation reaction is insufficient to populate directly the singlet state, the system may follow the “T-route” where the triplet state is first produced (reaction 7).



For such an “energy deficient system”, triplet-triplet recombination (reaction 8) may eventually yield the singlet emitting state in a second step. Both routes have been extensively studied with

various systems.<sup>34,35</sup> For the S-route, a simple two-level model shows that annihilation reaction should lead to the formation of 25% singlet  $^1A^*$  states and 75% triplet  $^3A^*$  states (Figure 6). This singlet/triplet ratio is due to spin statistics. In this case, we assume that the excited states of A are lower in energy than those for B, if A and B are not the same species. The species A is the energy acceptor in this process and it is the emissive species.

[Figure 6 near here]

For specific systems, it has been demonstrated that the emissive species is an *excimer* (*excited dimer*: dimer associated in an electronic excited state and dissociative in its ground state) or an *exciplex* (*excited complex*) formed by the annihilation reaction. A typical excimer example is pyrene.<sup>36</sup> The corresponding path is called “E-route” and emission occurs typically at much lower energies than the monomeric species.

The ECL annihilation pathway is very simple since it just requires the luminophore, solvent and supporting electrolyte to obtain ECL. However, both oxidized and reduced species should be generated in the same region near the electrode and this limits mainly this path to the use of organic solvents such as acetonitrile or DMF. Indeed, the potential window of water is not wide enough to form stable  $A^{\bullet-}$  and  $B^{\bullet+}$  species on most of the electrode materials.<sup>37</sup> In addition, the quenching effect and electroactivity of dioxygen is often encountered in annihilation ECL.

### 3.1.2. Coreactant pathway: a tandem system

If the reduced or oxidized form of the luminophore is not stable enough to produce ECL by annihilation, an alternative path (Scheme 2) based on the use of sacrificial reagents called coreactants has been progressively developed (Chapter 4). This pathway is very simple experimentally, because it just requires imposing a single potential step or sweeping the

potential in one direction. A coreactant can be defined as a chemical species that, upon electrochemical oxidation or reduction, produces very reactive intermediates capable to react with the oxidized or reduced luminophore to generate the desired excited state. The corresponding mechanisms are often referred to as “oxidative-reductive” and “reductive-oxidative” ECL, respectively. Typical coreactants are oxalate, TPrA, NADH, 2-(dibutylamino)ethanol (DBAE), peroxydisulfate, benzoyl peroxide (BPO), *etc.* The oxalate ion was the first ECL coreactant discovered in water and it follows an “oxidative-reductive” mechanism with the model ECL luminophore,  $[\text{Ru}(\text{bpy})_3]^{2+}$ . The oxalate anion  $\text{C}_2\text{O}_4^{2-}$  and the luminophore are first both oxidized at the electrode surface, generating  $\text{C}_2\text{O}_4^{\bullet-}$  and  $[\text{Ru}(\text{bpy})_3]^{3+}$ . Then, upon bond cleavage, the radical  $\text{C}_2\text{O}_4^{\bullet-}$  forms a strongly reducing radical  $\text{CO}_2^{\bullet-}$  that reduces  $[\text{Ru}(\text{bpy})_3]^{3+}$  and generates  $[\text{Ru}(\text{bpy})_3]^{2+*}$ , which emits ECL light at a typical wavelength. Therefore, for the “oxidative-reductive” mechanism, the sequence of reactions is as follow:

1. the electrochemical oxidations at the electrode surface;
2. bond-breaking (or atom-transfer) reaction of the coreactant giving a strong reducing radical;
3. the reduction of the oxidized luminophore by this radical produced from the coreactant.

The coreactant is a sacrificial molecule that is consumed irreversibly due to the bond-breaking reaction during the process whereas the luminophore is regenerated and ready to start a new ECL cycle. The role of the coreactant is to provide energetic radicals able to react with the luminophore in order to reach the excited state. When the annihilation pathway is not efficient, the coreactant pathway may give more intense ECL signals. It is interesting to notice that

oxidation of the coreactant engenders a strong reducing reagent after the chemical step. Amine-based coreactants such as TPrA, NADH or DBAE are widely used in aqueous solutions for bioanalytical applications. Most of the coreactant ECL applications are based on the “oxidative-reductive” scheme because it works very efficiently in water. An additional advantage of the coreactant approach is that ECL becomes possible even with some luminophores that do not have a stable reduced form.

In the “reductive-oxidative” pathway, both luminophore and coreactant are first reduced. The reduced form of the coreactant undergoes a chemical step, such as, for example, a bond cleavage, that generates a strong oxidizing radical. The electron-transfer reaction between the strong oxidizing coreactant radical and the reduced luminophore is then exergonic enough to populate the emissive state and to produce ECL. However, since cathodic potentials are required, hydrogen evolution dominates in aqueous solutions. Therefore, the electrogenerated species decompose too quickly to obtain a stable and reproducible ECL signal. In pure organic solvents or mixed acetonitrile/water solutions, the situation is different and stable ECL intensity may be generated by using adequate coreactants. BPO and peroxydisulfate are widely-used “reductive-oxidative” coreactants, which are very efficient in organic solvents.<sup>38-40</sup> They are reduced at the electrode surface and this first electrochemical step triggers the O-O bond cleavage, which forms strong oxidants  $\text{Ph-CO}_2^\bullet$  or  $\text{SO}_4^\bullet$ , respectively. These radicals resulting from the coreactant dissociation oxidize the reduced luminophore to generate the excited state.

To select efficient coreactants giving strong ECL intensity in this tandem luminophore/coreactant system, a number of criteria should be met: solubility in the considered medium, low reduction or oxidation potentials depending on the mechanistic pathways, stability, kinetics, quenching effects, toxicity, adequate redox potentials and sufficient lifetime of the radicals.

### 3.2. Bond-breaking reactions within the luminophore frame

The production of the excited state is not restricted to electron-transfer excitation reactions. A great variety of reactions involving a bond-breaking reaction or atom-transfer reaction within the luminophore frame itself has been reported.<sup>2, 41-44</sup> In this case, the bond-breaking reactions must be energetic enough to populate the emissive state. It implies that the electrochemiluminophore can emit a photon just once since it is a non-reversible reaction, on the contrary of the excitation electron-transfer reactions (*vide supra*). Typical examples are luminol, lucigenin (bis-N-methylacridinium nitrate), acridinium esters, etc. Luminol and its derivatives are probably the most popular ECL compounds belonging to this family of electrochemiluminophores.<sup>44-47</sup> In basic solutions, the oxidation of luminol in the presence of hydrogen peroxide produces an excited-state species, 3-aminophthalate. A simplified version of the ECL reactions of luminol is depicted on Figure 7. In aqueous alkaline solutions, luminol is oxidized at the electrode surface and forms a diazaquinone intermediate. This later reacts quantitatively with hydrogen peroxide, to produce the 3-aminophthalate in an excited state due to an O-O bond cleavage in the endoperoxide form. 3-Aminophthalate then emits a characteristic blue light at 425 nm. However, the quantum yield of the reaction is rather low ( $\sim 0.01$ ).<sup>42</sup>

[Figure 7 near here]

Different mechanistic pathways have been suggested depending on the applied electrode potentials.<sup>44, 48</sup> The inset in figure 7 shows that luminol ECL is produced at relatively mild oxidation potentials. In addition, the ECL intensity correlates directly with the amount of hydrogen peroxide. The luminol ECL method can be used to determine either luminol or species labeled with luminol or peroxides. Since hydrogen peroxide is an analyte of interest in various biological applications, this luminophore can measure reactive oxygen species (Chapter 16) in

the context of oxidative stress, for example. In addition, the enzymatic activity of oxidase-type enzymes, which generate hydrogen peroxide in the presence of their substrates can be monitored using luminol (Chapter 12). However, it is a non-renewable luminophore, which can produce ECL light just once.

### **3.3. Hot electron-induced ECL**

Hot electron-induced light emission is a special pathway in ECL. Hot electrons (a type of 'hot carriers') are electrons that have gained very high kinetic energy. Indeed, their energy is higher than the thermal energy of the solution or the Fermi level in solution. The injection of hot electrons into electrolyte solution from an oxide covered electrode surface can thus be utilized to produce ECL.<sup>49-51</sup> Usually, the insulating layer of metal oxide prevents the electron-transfer reaction from the metal to a species dissolved in the solution. However, in the presence of a large electric field across the oxide layer and with the Fermi level in the metal above the conduction band of the metal oxide, hot electrons can be injected into aqueous electrolyte solution from thin insulating film coated electrodes. These surfaces behave as cathodes due to the strong reductive capacity of the injected hot electrons. This pathway allows ECL detection of  $[\text{Ru}(\text{bpy})_3]^{2+}$  and luminol.<sup>49, 50</sup>

## **4. Key protagonists in the ECL**

The annihilation pathway is conceptually very simple because the only chemical species involved is the luminophore that is submitted alternately to an oxidation and a reduction. This necessitates the use of an AC input at a reasonably high frequency to enable the presence of the electro-oxidized and electro-reduced forms of the luminophore. Therefore, both electrogenerated species should be sufficiently stable at the timescale of the AC switch. Unfortunately, only a limited number of luminophores are ECL-active according to this

pathway, which requires the use of rigorously purified and deoxygenated organic solvents and supporting electrolytes. Indeed, the available potential window is usually too narrow in aqueous solutions to enable the generation of the stable oxidized and/or reduced forms. Practically, the alternative strategy that employs a suitable sacrificial coreactant in combination with a given luminophore is the most widely investigated one.

## 4.1. Luminophores

From an historical point of view, the first luminophores that were reported as chemiluminescent during an electrolysis were Grignard compounds (formula  $\text{RMgX}$  where X stands for a halogen atom)<sup>9</sup> and luminol.<sup>10</sup> Potentially, any kind of luminophore suitable for CL can be employed in ECL. Nowadays three main classes of luminophores can be distinguished: organic, inorganic (i.e. transition metal complexes) and nanoparticles or clusters (Chapters 3, 9, 10 and 11). All these ECL-active luminophores have been extensively reviewed in the past.<sup>2, 3, 41, 52</sup> Classic organic luminophores are aromatic and feature 5- or 6- member rings containing carbon and/or various heteroatoms such as N, O, S, etc. During the early 60's, when the initial ECL observations were re-investigated and rationalized, anthracene, perylene or rubrene derivatives were extensively studied.<sup>13, 14</sup> ECL based on many inorganic complexes were also widely exemplified with period 4 (Cr, Cu...), 5 (Mo, Ru, Rh...) and 6 (Re, Os, Ir, Pt...) elements.<sup>41</sup> Several lanthanide-based metal complexes were also reported. Such a large range of luminophores offers the possibility to select the luminophore with a given emission wavelength spanning across the visible region and up to the near infrared. Practically, the most frequent ECL luminophore remains  $[\text{Ru}(\text{bpy})_3]^{2+}$  that is the gold standard reference.

A strategy that has recently been proposed is based on the co-employment of two luminophores that exhibit different redox potentials (Chapter 8). By tuning the applied potential, it is then possible to activate either one or both of them simultaneously. Such a concept was proposed

with a conventional electrochemical setup<sup>53</sup> and also in the framework of bipolar electrochemistry in either open- or closed-configurations (Chapter 7).<sup>54-56</sup>

The last category of luminophores are nanoparticles or quantum dots. In that case, the strategy consists to inject excitons either in the valence or conduction band of the particles (Figure 8). Anodic and cathodic ECL were proposed in that context by choosing an appropriate coreactant.

[Figure 8 near here]

The first particles described were Si nanocrystals and CdSe quantum dots.<sup>57, 58</sup> Their electronic properties are primarily controlled by the size and also the surface state of these particles. Other quantum dots such as ZnSe or CdS are also ECL-active.<sup>59, 60</sup> Carbon-based nanoparticles are equally suitable as exemplified by carbon nanocrystals or graphene.<sup>61, 62</sup> Finally, atomically precise noble metal clusters constituted only by a few atoms were successfully investigated as ECL luminophores.<sup>63, 64</sup>

## 4.2. Coreactants

As stated above, under specific conditions, the use of a luminophore without any supplementary chemicals can enable ECL by electrogenerating at a sufficient frequency (pulsed potential) both the oxidized and reduced forms that self-annihilate in the reaction layer close to the electrode surface. However, this strategy necessitates a relative stability of all the implied redox states in the considered solvent and is only convenient for a limited number of luminophores. This is why a sacrificial coreactant is usually added in order to achieve ECL when applying a single potential step. Such an experimental strategy is in fact rather counter-intuitive because the ECL phenomenon is driven by exergonic redox chemistry that necessitate the simultaneous presence of strong oxidizing and reducing species. Therefore, a suitable coreactant should produce a strong reductant after an initial oxidation step followed by a chemical reaction or reciprocally a strong oxidant after a reduction step and a chemical reaction. This means that in all cases the



electron-transfer step is coupled with a subsequent chemical reaction. Typically, the latter step comprises a bond cleavage and is therefore irreversible. Even if this kind of chemicals is quite rare, the two most employed candidates are amines and peroxides. A model mechanism for each class of compound is depicted in Scheme 3.

For an “oxidative-reduction” mechanism, amines are very appropriate coreactants. The oxidation of an amine leads to the formation of a radical cation. In that case, a proton in position  $\alpha$  with respect to the charge is rather acidic, facilitating thus the corresponding dissociation. This irreversible bond cleavage affords a strongly reactive radical (Scheme 3a). In fact, the reactivity of the amine depends on the electronic environment surrounding the charge that can stabilize or destabilize the electrogenerated cation radical. In that context, TPrA serves as a reference coreactant and the redox potential of the corresponding TPrA $^{\bullet}$  was reported to be  $-1.7$  V *vs.* Ag/AgCl.<sup>65</sup> If used in combination with [Ru(bpy)<sub>3</sub>]<sup>2+</sup>, which is oxidized in water at  $+1$  V *vs.* Ag/AgCl, the corresponding annihilation reaction yields more than 2.7 eV. This value is more than enough to drive red light emission ( $\lambda = 620$  nm) of the luminophore.

[Scheme 3 near here]

On the contrary, an efficient coreactant for the “reductive-oxidation” path can be exemplified with peroxides. In that case, the coreactant is reduced to form the corresponding radical anion (Scheme 3b). Then, the O–O single bond undergoes a homolytic cleavage leading to a carboxylate anion and a strong oxidant radical. According to this strategy, BPO is very widely used because its mild reduction conditions provide a radical exhibiting a redox potential of  $\sim 1.5$  V *vs.* SCE as measured from the irreversible oxidation of benzoate.<sup>30, 66</sup> It is noteworthy that, depending on the nature of the coreactant, the redox potential of the chemical species formed after a dissociative electron-transfer is not always easy to determine. Therefore, there is sometimes a discrepancy in the corresponding redox potential values reported in the literature.

A good way to rationalize this could be to test a series of luminophores exhibiting various emission wavelengths employed in ECL with the same coreactant.

### **4.3. Electrode materials**

In ECL, as with all electrochemical processes, a special attention should be given to the nature of the electrode materials (Chapter 6). The reason is simply because the light emission is triggered by heterogeneous electron-transfer reactions that are indeed strongly influenced by the chemical nature of the electrode. The experimenter has typically to choose between metal electrodes (Au, Pt, etc.), carbon ones (glassy carbon, boron-doped diamond, etc.) or semiconducting oxides (indium tin oxide, fluorine-doped tin oxide, etc.). All these electrode materials have respective advantages and drawbacks that should be considered prior to being used in ECL.

## **5. Analytical applications**

### **5.1. Analytical strategies**

ECL is an outstanding transduction mode in analytical sensing. This is primarily due to the simple visual readout provided by ECL and the signal over noise level that is extremely low compared to photoluminescence, since the excitation does not involve photon absorption in ECL.

Historically, the first molecular targets detected through ECL were the luminophore and/or the coreactant in order to demonstrate the analytical feasibility. The strength of the ECL emission is indeed very much dependent on the concentrations of these two protagonists.<sup>22, 27, 67-70</sup> Several classic coreactants were quantified in combination with  $[\text{Ru}(\text{bpy})_3]^{2+}$  as a luminophore. This was exemplified with oxalate, peroxydisulfate or various amines.<sup>68, 71, 72</sup> Besides model coreactants, the same strategy was also applied to detect biorelevant molecules that feature

amine groups. For example, anesthetic drugs such as lidocaine or NADH were successfully determined.<sup>72, 73</sup> The influence of additional chemicals can also influence the ECL intensity usually by means of molecular quenching or more rarely enhancement. In this context, phenols and quinones can be cited as quenchers whereas halides can increase the ECL signal under certain circumstances.<sup>74, 75</sup>

Luminophore sensing by itself is not very useful because in most cases these dyes are not chemically or biochemically relevant. However, the ECL signal being concentration-dependent, the luminophore can act as an ECL label, providing thus an interesting analytical strategy. In that context,  $[\text{Ru}(\text{bpy})_3]^{2+}$  is extensively used to label various biomolecules for ready-to-use titration kits. Functional versions of this dye bearing reactive groups such as activated esters are also readily available from chemical companies. In the latter cases, the luminophore can be used indifferently in solution or surface-immobilized while the ECL signal is recorded in presence of a large excess of coreactant (generally TPrA). These conditions allow ECL signaling that is strictly sensitive to the dye content.

## 5.2. Bioassays

Over the years, ECL has found many possible analytical applications. They can be essentially divided into four different types: immunoassays, DNA, aptamers and enzymatic sensing (Chapters 12-15).

Bard and Whitesides patented the groundbreaking idea describing ECL immunoassays (ECLIA).<sup>28</sup> The strategy takes advantage of a ruthenium ECL label bearing a NHS activated ester, enabling to target many different biomacromolecules. ECL immunosensing is typically carried out in a solid-phase format offering many possibilities such as a direct or competitive detection and also the classic sandwich mode using primary and secondary antibodies (Chapter

15). The predominant format of ECL bioassays that are commercially available takes advantage of a magnetic solid support (i.e. magnetic beads) to facilitate the immobilization step at the surface of the electrode by using an external magnet (Figure 9).<sup>76</sup> Two other key-advantages are achieved when selecting microscale magnetic beads. First, a much greater surface area is obtained during the sensing step compared to a flat surface and this assay is very often considered as being homogeneous. Secondly, the size of the bead can be adjusted in order to control the distance towards the electrode and maximize the ECL intensity during the reporting step. This dimension is indeed crucial to maintain the ECL label in close proximity of the electrode surface where the concentration of the electrogenerated TPrA radicals are optimal. A typical size of 3  $\mu\text{m}$  appears to be adequate for ECL sandwich immunoassays.<sup>65, 77, 78</sup> Nowadays, about 150 bioassays are available for various pathologies including cardiac disease, tumor markers, bone markers, infectious disease, thyroid function tests, anemia and fertility tests (commercialized by Roche Diagnostics Inc. and Meso Scale Discovery Inc.).

[Figure 9 near here]

DNA is also an essential biological target that can be detected by ECL technology (Chapters 13 and 14). The vast majority of these ECL-based DNA sensing takes advantage of a label as for immunoassays.<sup>79</sup> However, targeting DNA allows also combining advantageously the ECL detection mode with a mediated amplification step. Such a coupling affords ultimately very low limits of detection where only a couple a copies of the DNA target are present in the sample. The main goal is currently to combine nanostructured materials that exhibit large surface areas for grafting and recognition with DNA amplification techniques such as polymerase chain reaction (PCR), hybridization chain reaction (HCR), rolling-circle amplification (RCA), loop-mediated isothermal amplification (LAMP), etc.

More recently, an aptamer-based strategy was widely adapted to ECL assay. Aptamers are single-stranded DNA that can fold in a well-defined 3-dimensional structure being able to recognize very specifically a given target. The nucleic acid sequence is established following a combinatorial chemistry approach called systematic evolution of ligands by exponential enrichment (SELEX). This specific molecular recognition is adaptable to almost any chemical or biochemical targets ranging from small molecules to large proteins. Among all possibilities, the detection of thrombin is considered as a benchmark system that can be used to test ECL detection protocols.<sup>80</sup> Regardless the immobilization strategy and/or eventual amplification, steps, the common idea is very often the modulation of the distance between the ECL label and the surface upon probe/target recognition. Additionally, numerous strategies based on quenching were also proposed.

ECL transduction is widely used for monitoring enzymatic reactions (Chapter 12). A key-strategy involves one of the enzymatic protagonist (reactant, product, co-factor) acting also as co-reactant for the ECL reaction. Depending on the enzymatic reactivity, several possibilities can be distinguished.<sup>81</sup> With the large family of dehydrogenases that can convert many different substrates, NAD<sup>+</sup> coenzyme is converted into NADH. This latter can act as ECL coreactant with [Ru(bpy)<sub>3</sub>]<sup>2+</sup> luminophore. In that case, a classic biorelevant substrate is glucose.<sup>82</sup> Secondly, many oxidases use molecular oxygen as electron acceptor and readily produce hydrogen peroxide. Therefore, luminol dye is well-adapted to detect such an enzymatic activity as the ECL strength is H<sub>2</sub>O<sub>2</sub> concentration-dependent.<sup>83</sup>

## 5. Conclusion

ECL is by essence a multidisciplinary field since it combines electrochemical addressing and orthogonal optical detection modalities. Thus, ECL covers several fields from electrochemistry to photophysics, photochemistry, material chemistry, nanosciences, organic chemistry,

analytical chemistry, biochemistry, *etc.* In this introductory chapter, the emphasis has been on the basics that are required to understand the more specific topics that are developed in the following chapters. It is amazing to realize how ECL has evolved from a “laboratory curiosity” to a powerful analytical technique. The results of the fundamental research on electron-transfer reactions performed initially in organic solvents under drastic conditions are routinely exploited to generate ECL in aqueous media at physiological pH nowadays. Such experiments can be performed easily in any particular chemical or biological laboratory. ECL technology is successfully commercialized for the diagnostic market thanks to its intrinsic remarkable properties

## References

1. A. J. Bard and L. R. Faulkner, *Electrochemical methods*, Wiley, New York, 2001.
2. W. Miao, *Chem. Rev.*, 2008, **108**, 2506-2553.
3. Z. Liu, W. Qi and G. Xu, *Chem. Soc. Rev.*, 2015, **44**, 3117-3142.
4. A. J. Bard, *Electrogenerated Chemiluminescence*, M. Dekker, New-York, 2004.
5. S. Parveen, M. S. Aslam, L. Hu and G. Xu, *Electrogenerated Chemiluminescence. Protocols and Applications*, Springer, 2013.
6. M. Hesari and Z. Ding, *J. Electrochem. Soc.*, 2016, **163**, H3116-H3131.
7. L. R. Faulkner and A. J. Bard, in *Electroanalytical chemistry*, ed. A. J. Bard, M. Dekker, New-York, 1977, vol. 10, pp. 1-95.
8. B. Valeur, *Molecular Fluorescence: Principles and Applications*, Wiley-VCH, 2001.
9. R. T. Dufford, D. Nightingale and L. W. Gaddum, *J. Am. Chem. Soc.*, 1927, **49**, 1858-1864.
10. N. Harvey, *J. Phy. Chem.*, 1928, **33**, 1456-1459.
11. E. A. Chandross and F. I. Sonntag, *J. Am. Chem. Soc.*, 1964, **86**, 3179-3180.
12. D. M. Hercules, *Science*, 1964, **145**, 808-809.
13. R. E. Visco and E. A. Chandross, *J. Am. Chem. Soc.*, 1964, **86**, 5350-5351.
14. K. S. V. Santhanam and A. J. Bard, *J. Am. Chem. Soc.*, 1965, **87**, 139-140.
15. D. M. Hercules and F. E. Lytle, *J. Am. Chem. Soc.*, 1966, **88**, 4745-4746.
16. N. E. Tokel and A. J. Bard, *J. Am. Chem. Soc.*, 1972, **94**, 2862-2863.
17. M.-M. Chang, T. Saji and A. J. Bard, *J. Am. Chem. Soc.*, 1977, **99**, 5399-5403.
18. E. A. Chandross, *Tetrahedron Lett.*, 1963, **4**, 761-765.
19. F. Bolletta, A. Rossi and V. Balzani, *Inorg. Chim. Acta*, 1981, **53**, L23-L24.
20. H. S. White and A. J. Bard, *J. Am. Chem. Soc.*, 1982, **104**, 6891-6895.
21. J. B. Noffsinger and N. D. Danielson, *Anal. Chem.*, 1987, **59**, 865-868.
22. J. K. Leland and M. J. Powell, *J. Electrochem. Soc.*, 1990, **137**, 3127-3131.
23. R. A. Marcus, *J. Chem. Phys.*, 1965, **43**, 2654-2657.
24. A. Kapturkiewicz, in *Advances in electrochemical science and engineering*, eds. R. C. Alkire, H. Gerischer, D. M. Kolb and C. W. Tobias, Wiley-VCH, vol. 5, pp. 1-60.

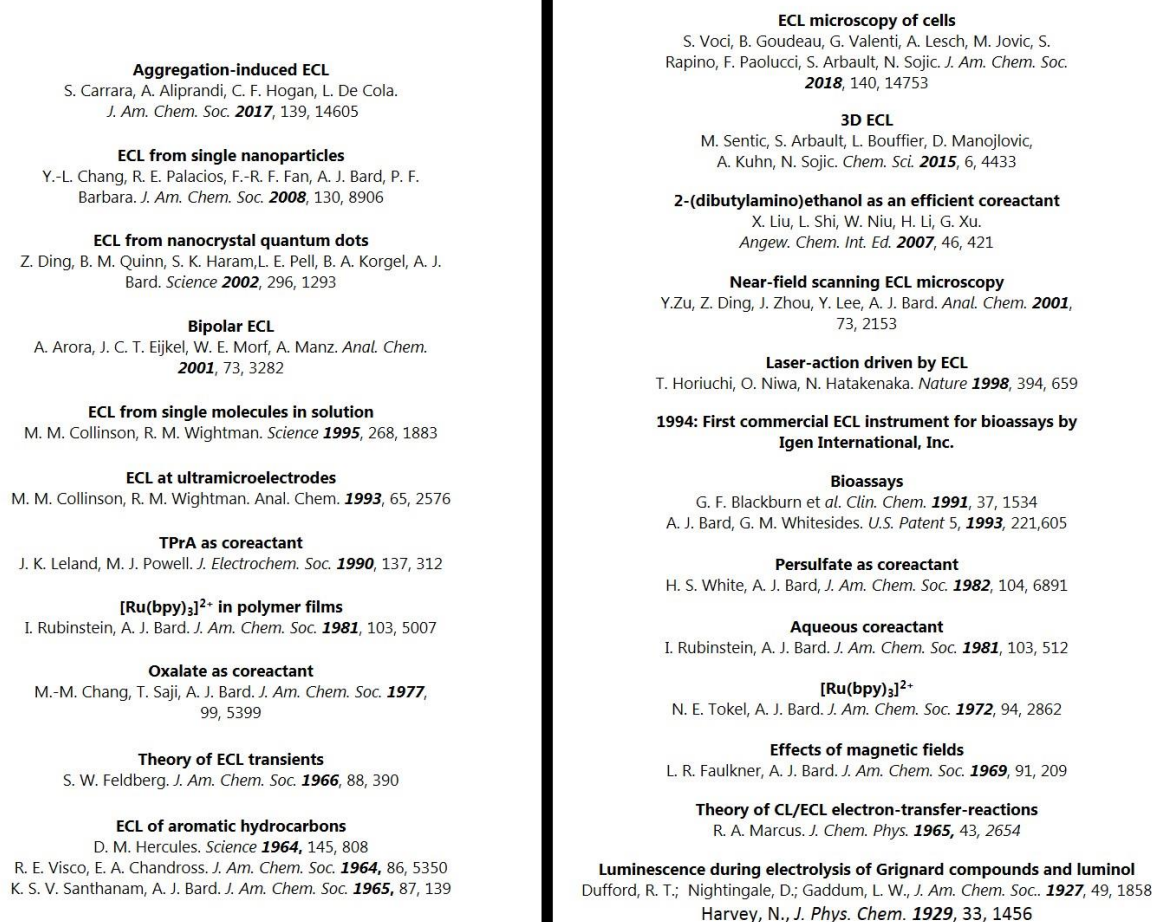
25. R. A. Marcus, *Angew. Chem. Int. Ed.*, 1993, **32**, 1111-1121.
26. I. Rubinstein and A. J. Bard, *J. Am. Chem. Soc.*, 1981, **103**, 512-516.
27. G. F. Blackburn, H. P. Shah, J. H. Kenten, J. Leland, R. A. Kamin, J. Link, J. Peterman, M. J. Powell, A. Shah, D. B. Talley, S. K. Tyagi, E. Wilkins, T.-G. Wu and R. J. Massey, *Clin. Chem.*, 1991, **37**, 1534-1539.
28. A. J. Bard and G. M. Whitesides, *U.S. Patent* 1993, 5,238,808.
29. J. Heinze, *Angew. Chem. Int. Ed.*, 1984, **23**, 831-847.
30. S. Antonello and F. Maran, *J. Am. Chem. Soc.*, 1999, **121**, 9668-9676.
31. B. D. Stringer, L. M. Quan, P. J. Barnard, D. J. D. Wilson and C. F. Hogan, *Organometallics*, 2014, **33**, 4860-4872.
32. H. Li, S. Voci, A. Wallabregue, C. Adam, G. M. Labrador, R. Duwald, I. Hernández Delgado, S. Pascal, J. Bosson, J. Lacour, L. Bouffier and N. Sojic, *ChemElectroChem*, 2017, **4**, 1750-1756.
33. A. Kapturkiewicz, *ChemElectroChem*, 2017, **4**, 1604-1638.
34. L. R. Faulkner and A. J. Bard, *J. Am. Chem. Soc.*, 1968, **90**, 6284.
35. R. S. Glass and L. R. Faulkner, *J. Phys. Chem.*, 1981, **85**, 1160-1165.
36. B. Fleet, G. F. Kirkbright and C. J. Pickford, *J. Electroanal. Chem.*, 1971, **30**, 115-121.
37. G. Valenti, A. Fiorani, H. Li, N. Sojic and F. Paolucci, *ChemElectroChem*, 2016, **3**, 1990-1997.
38. D. L. Akins and R. L. Birke, *Chem. Phys. Lett.*, 1974, **29**, 428-435.
39. A. Fiorani, Irkham, G. Valenti, F. Paolucci and Y. Einaga, *Anal. Chem.*, 2018, **90**, 12959-12963.
40. H. S. White, W. G. Becker and A. J. Bard, *J. Phys. Chem.*, 1984, **88**, 1840-1846.
41. M. M. Richter, *Chem. Rev.*, 2004, **104**, 3003-3036.
42. C. Marquette and L. Blum, *Anal. Bioanal. Chem.*, 2008, **390**, 155.
43. Y.-G. Sun, H. Cui and X.-Q. Lin, *J. Lumin.*, 2001, **92**, 205-211.
44. S. Sakura, *Anal. Chim. Acta*, 1992, **262**, 49-57.
45. K. Arai, K. Takahashi and F. Kusu, *Anal. Chem.*, 1999, 2237-2240.
46. F. Han, H. Jiang, D. Fang and D. Jiang, *Anal. Chem.*, 2014, **86**, 6896-6902.
47. Y. Liu, W. Shen, Q. Li, J. Shu, L. Gao, M. Ma, W. Wang and H. Cui, *Nat. Commun.*, 2017, **8**, 1003.
48. X. Q. Lin, G. Sun and H. Cui, *Chinese J. Anal. Chem.*, 1999, **27**, 497.
49. S. Kulmala, T. Ala-Kleme, A. Kulmala, D. Papkovsky and K. Loikas, *Anal. Chem.*, 1998, **70**, 1112-1118.
50. T. Ala-Kleme, S. Kulmala, L. Vare, P. Juhala and M. Helin, *Anal. Chem.*, 1999, **71**, 1999, 1971, 5538-5543.
51. F. Gaillard, Y.-E. Sung and A. J. Bard, *J. Phys. Chem. B*, 1999, **103**, 667-674.
52. P. Wu, X. Hou, J.-J. Xu and H.-Y. Chen, *Chem. Rev.*, 2014, **114**, 11027-11059.
53. E. H. Doeven, E. M. Zammit, G. J. Barbante, C. F. Hogan, N. W. Barnett and P. S. Francis, *Angew. Chem. Int. Ed.*, 2012, **51**, 4354-4357.
54. H. Li, L. Bouffier, S. Arbault, A. Kuhn, C. F. Hogan and N. Sojic, *Electrochem. Commun.*, 2017, **77**, 10-13.
55. M. R. Moghaddam, S. Carrara and C. F. Hogan, *Chem. Commun.*, 2019, **55**, 1024-1027.
56. Y.-Z. Wang, S.-Y. Ji, H.-Y. Xu, W. Zhao, J.-J. Xu and H.-Y. Chen, *Anal. Chem.*, 2018, **90**, 3570-3575.
57. Z. Ding, B. M. Quinn, S. K. Haram, L. E. Pell, B. A. Korgel and A. J. Bard, *Science*, 2002, **296**, 1293-1297.
58. N. Myung, Z. Ding and A. J. Bard, *Nano Lett.*, 2002, **2**, 1315-1319.
59. N. Myung, Y. Bae and A. J. Bard, *Nano Lett.*, 2003, **3**, 1053-1055.
60. G. Jie, B. Liu, H. Pan, J.-J. Zhu and H.-Y. Chen, *Anal. Chem.*, 2007, **79**, 5574-5581.
61. L. Zheng, Y. Chi, Y. Dong, J. Lin and B. Wang, *J. Am. Chem. Soc.*, 2009, **131**, 4564-4565.
62. L.-L. Li, J. Ji, R. Fei, C.-Z. Wang, Q. Lu, J.-R. Zhang, L.-P. Jiang and J.-J. Zhu, *Adv. Funct. Mat.*, 2012, **22**, 2971-2979.

63. K. N. Swanick, M. Hesari, M. S. Workentin and Z. Ding, *J. Am. Chem. Soc.*, 2012, **134**, 15205-15208.
64. M. Hesari, M. S. Workentin and Z. Ding, *ACS Nano*, 2014, **8**, 8543-8553.
65. W. Miao, J.-P. Choi and A. J. Bard, *J. Am. Chem. Soc.*, 2002, **124**, 14478-14485.
66. S. Antonello and F. Maran, *J. Am. Chem. Soc.*, 1997, **119**, 12595-12600.
67. A. J. Bard, J. D. Debad, J. K. Leland, G. B. Sigal, J. L. Wilbur and J. N. Wohlstadter, in *Encyclopedia of Analytical Chemistry: Applications, Theory and Instrumentations*, ed. Meyers, Wiley, 2000, vol. 11, pp. 9842-9849.
68. I. Rubinstein, C. R. Martin and A. J. Bard, *Anal. Chem.*, 1983, **55**, 1580-1582.
69. D. Ege, W. G. Becker and A. J. Bard, *Anal. Chem.*, 1984, **56**, 2413-2417.
70. S. A. Cruser and A. J. Bard, *Anal. Lett.*, 1967, **1**, 11-17.
71. K. Yamashita, S. Yamazaki-Nishida, Y. Harima and A. Segawa, *Anal. Chem.*, 1991, **63**, 872-876.
72. A. W. Knight and G. M. Greenway, *Analyst*, 1996, **121**, 101R-106R.
73. M. Milutinovic, S. Sallard, D. Manojlovic, N. Mano and N. Sojic, *Bioelectrochem.*, 2011, **82**, 63-68.
74. J. McCall, C. Alexander and M. M. Richter, *Anal. Chem.*, 1999, **71**, 2523-2527.
75. Y. Zu and A. J. Bard, *Anal. Chem.*, 2000, **72**, 3223-3232.
76. X. Zhou, D. Zhu, Y. Liao, W. Liu, H. Liu, Z. Ma and D. Xing, *Nat. Protocols*, 2014, **9**, 1146-1159.
77. M. Sentic, M. Milutinovic, F. Kanoufi, D. Manojlovic, S. Arbault and N. Sojic, *Chem. Sci.*, 2014, **5**, 2568-2572.
78. Y. Wei, Y. Wang, J. Wang, X. Yang, H. Qi, Q. Gao, C. J. A. Zhang and B. Chemistry, *Anal. Bioanal. Chem.*, 2019, DOI: 10.1007/s00216-019-01830-1.
79. W. Miao and A. J. Bard, *Anal. Chem.*, 2003, **75**, 5825-5834.
80. X.-B. Yin, *TrAC, Trends Anal. Chem.*, 2012, **33**, 81-94.
81. X.-M. Chen, B.-Y. Su, X.-H. Song, Q.-A. Chen, X. Chen and X.-R. Wang, *Trends Anal. Chem.*, 2011, **30**, 665-676.
82. A. F. Martin and T. A. Nieman, *Biosens. Bioelectron.*, 1997, **12**, 479-489.
83. C. A. Marquette and L. J. Blum, *Anal. Bioanal. Chem.*, 2006, **385**, 546-554.

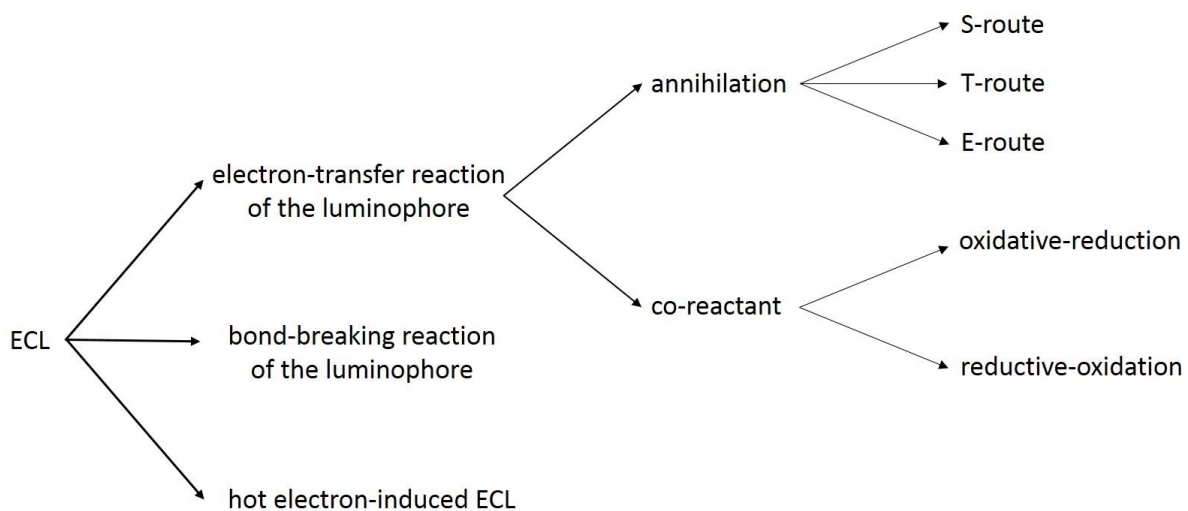


Table 1. Different types of luminescence

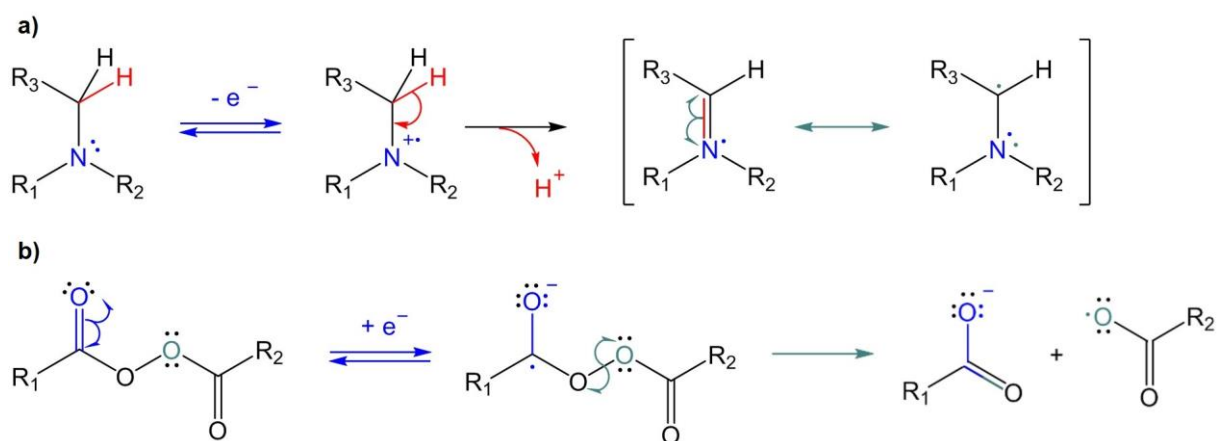
Luminescence type	initiated or caused by
Photoluminescence (fluorescence, phosphorescence)	Absorption of photons
Chemiluminescence	Chemical reaction
Bioluminescence	Biochemical reactions in a living organism
Electrogenerated chemiluminescence	Electrochemical reaction
Electroluminescence	Radiative recombination of electrons and holes in a material
Crystalloluminescence	Crystallization reaction
Lyoluminescence,	Dissolution of a solid in a solvent
Sonoluminescence	Imploding bubbles in a liquid when excited by sound
Mechanoluminescence	Mechanical action on a solid



Scheme 1. Timeline for the development of different new concepts and applications in ECL.



Scheme 2. Different mechanistic pathways giving ECL.



Scheme 3. Sequence of chemical reorganization following the initial electron-transfer reactions for a) TPrA and b) BPO.

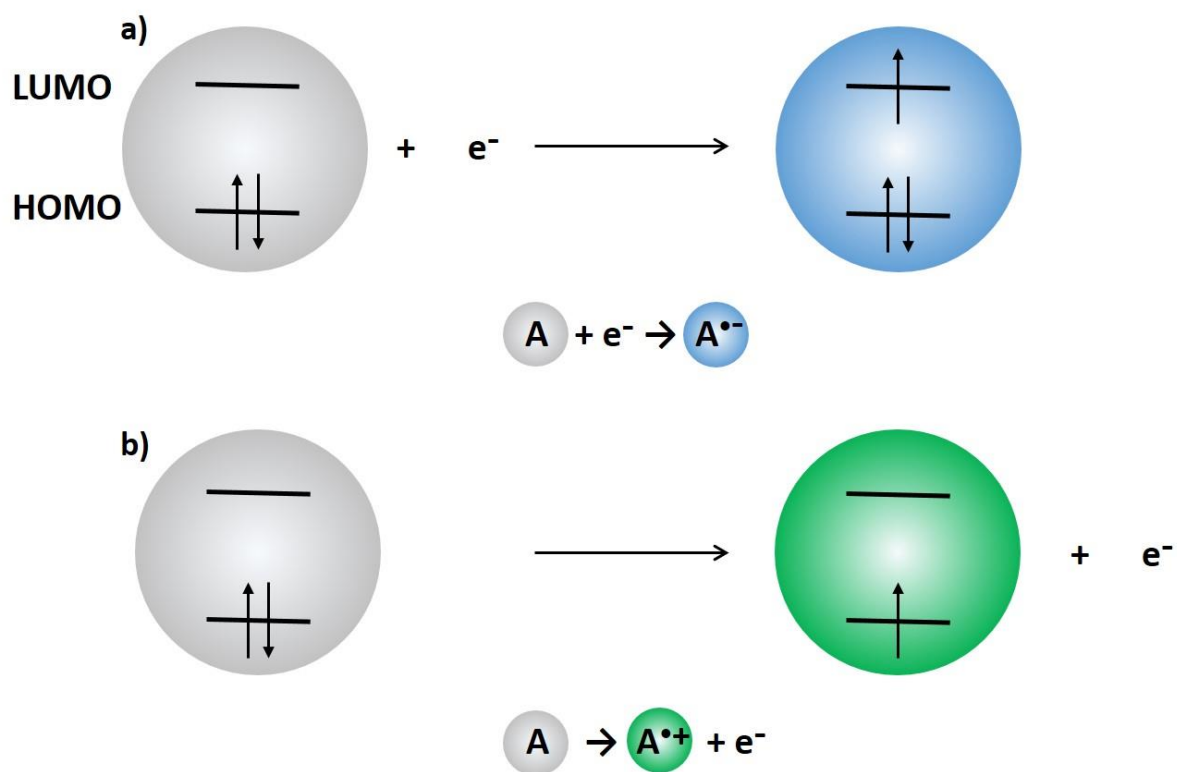


Figure 1. Schematic representation of a) reduction and b) oxidation reactions involving the LUMO and HOMO, respectively.

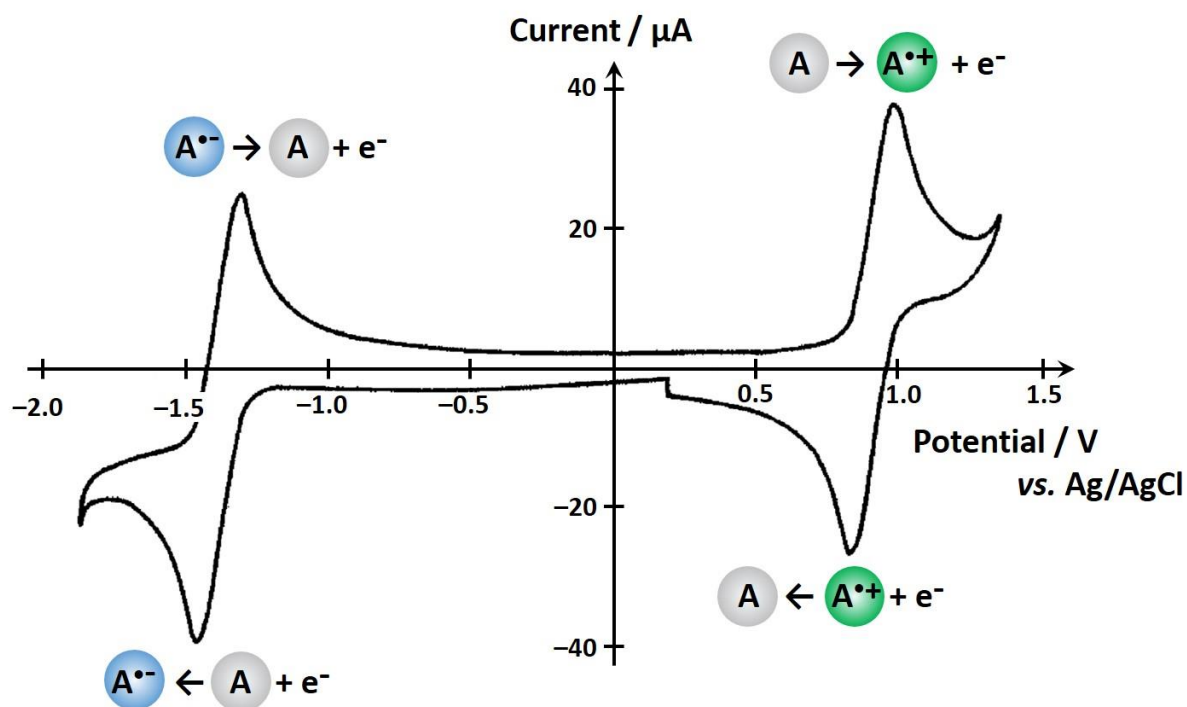


Figure 2. Typical cyclic voltammogram for a reversible species that forms stable reduced and oxidized ions during the timescale of the experiments. Cyclic voltammetric curve of 0.6 mM rubrene in benzonitrile with 0.1 M tetra-*n*-butylammonium perchlorate as supporting electrolyte.

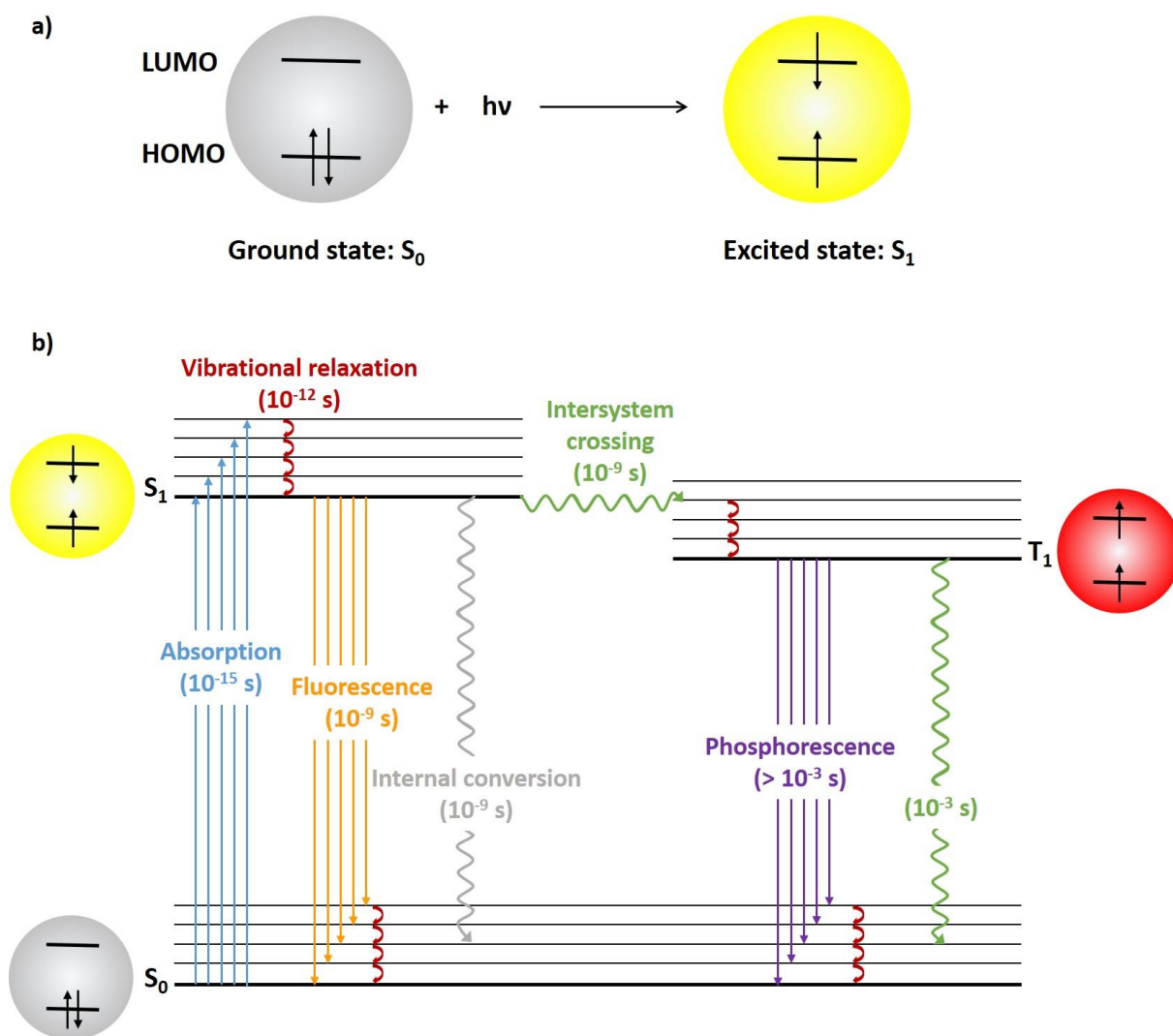


Figure 3. a) Schematic view showing the general principles of photoluminescence with the representation of the molecular orbitals. b) Jablonski diagram representing the typical photophysical processes in molecules. The time constants should be considered as typical orders of magnitude.

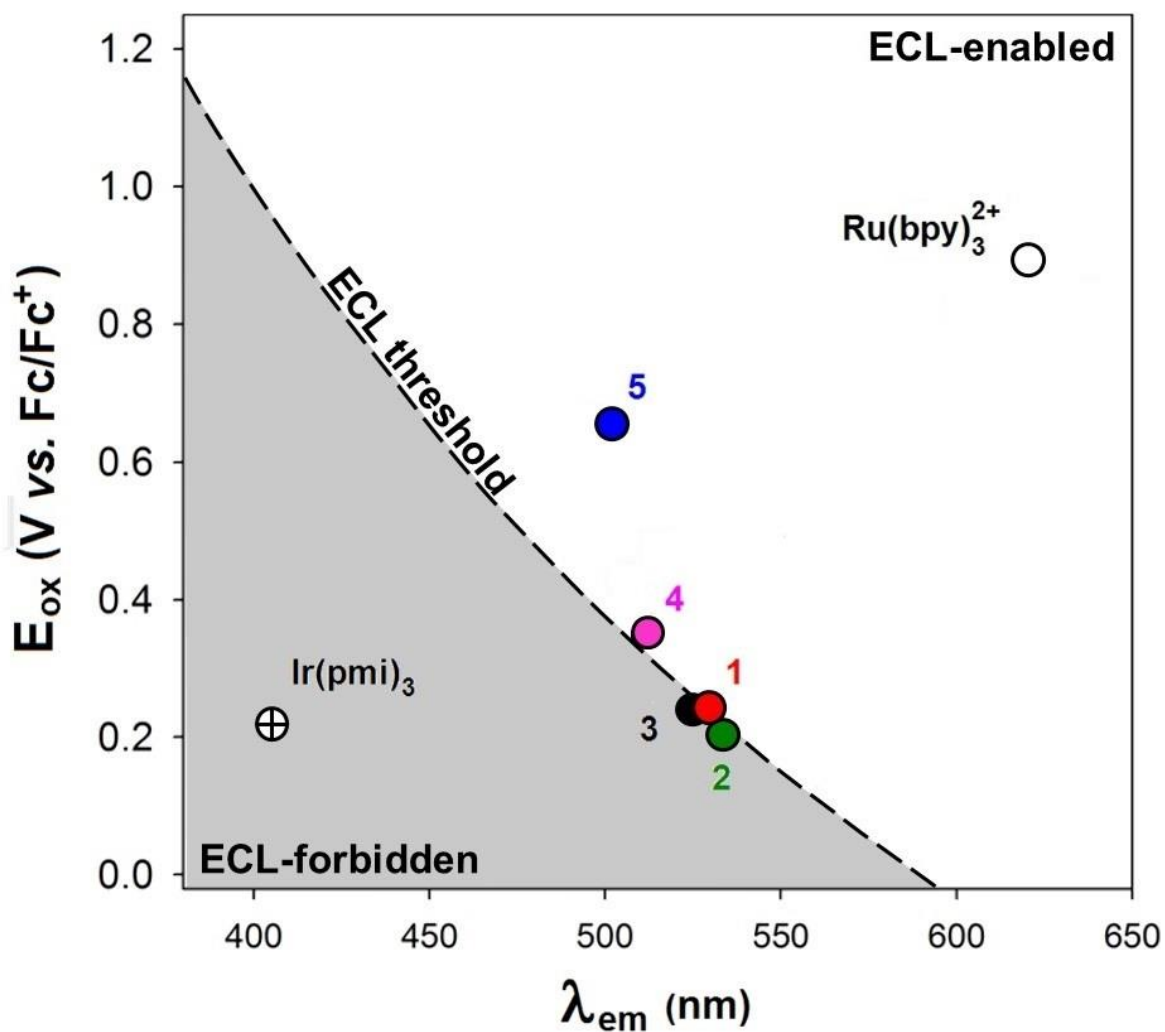


Figure 4. Zone diagram illustrating the energetic criterion for formation of the excited state of a series of iridium complexes labelled from 1 to 5 and two reference inorganic dyes.<sup>31</sup>



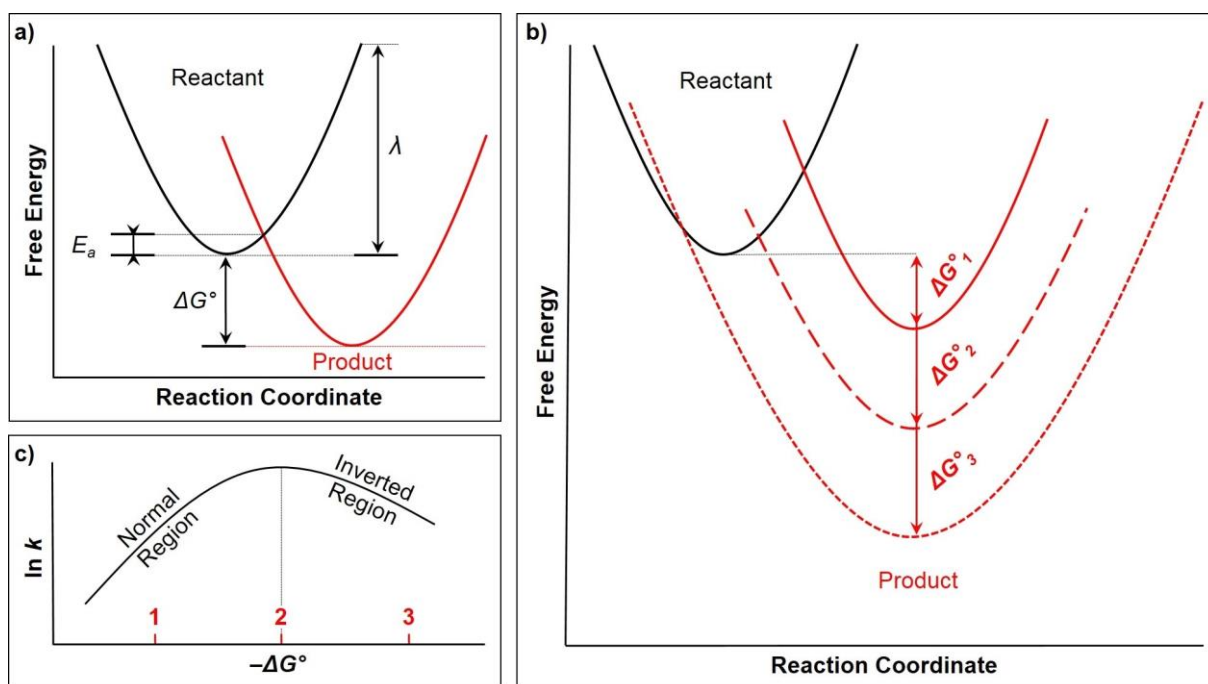


Figure 5. a) Graphic displaying the free energy in function of the reaction coordinate. The potential energy curves of the reactant and product are the black and red parabolas, respectively. The three key parameters (activation energy, Gibbs energy and reorganization energy) are linked together according to Marcus theory. b) Influence of the Gibbs energy on the potential surface of the product. c) Relationship between the logarithm of the rate constant and the opposite of the Gibbs energy that delimits the normal and inverted regions of Marcus theory.<sup>25</sup>

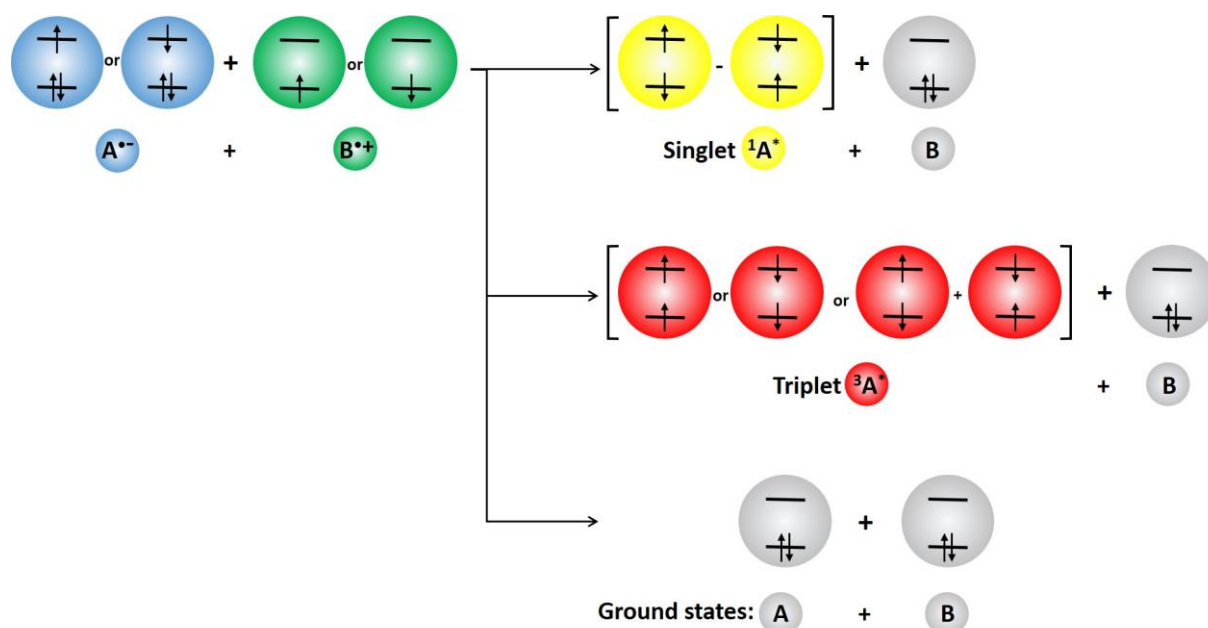


Figure 6. a) Schematic representation of the bimolecular electron-transfer reaction between the radical species  $A^{\bullet-}$  and  $B^{\bullet+}$ . For energy-sufficient reaction, spin statistics dictate the singlet/triplet ration with the formation of 25% singlet states  $^1A^*$  (spins antiparallel with zero resultant spin angular momentum) and 75% triplet states  $^3A^*$  (spins parallel, with three resulting nonzero spin angular momentum vectors).

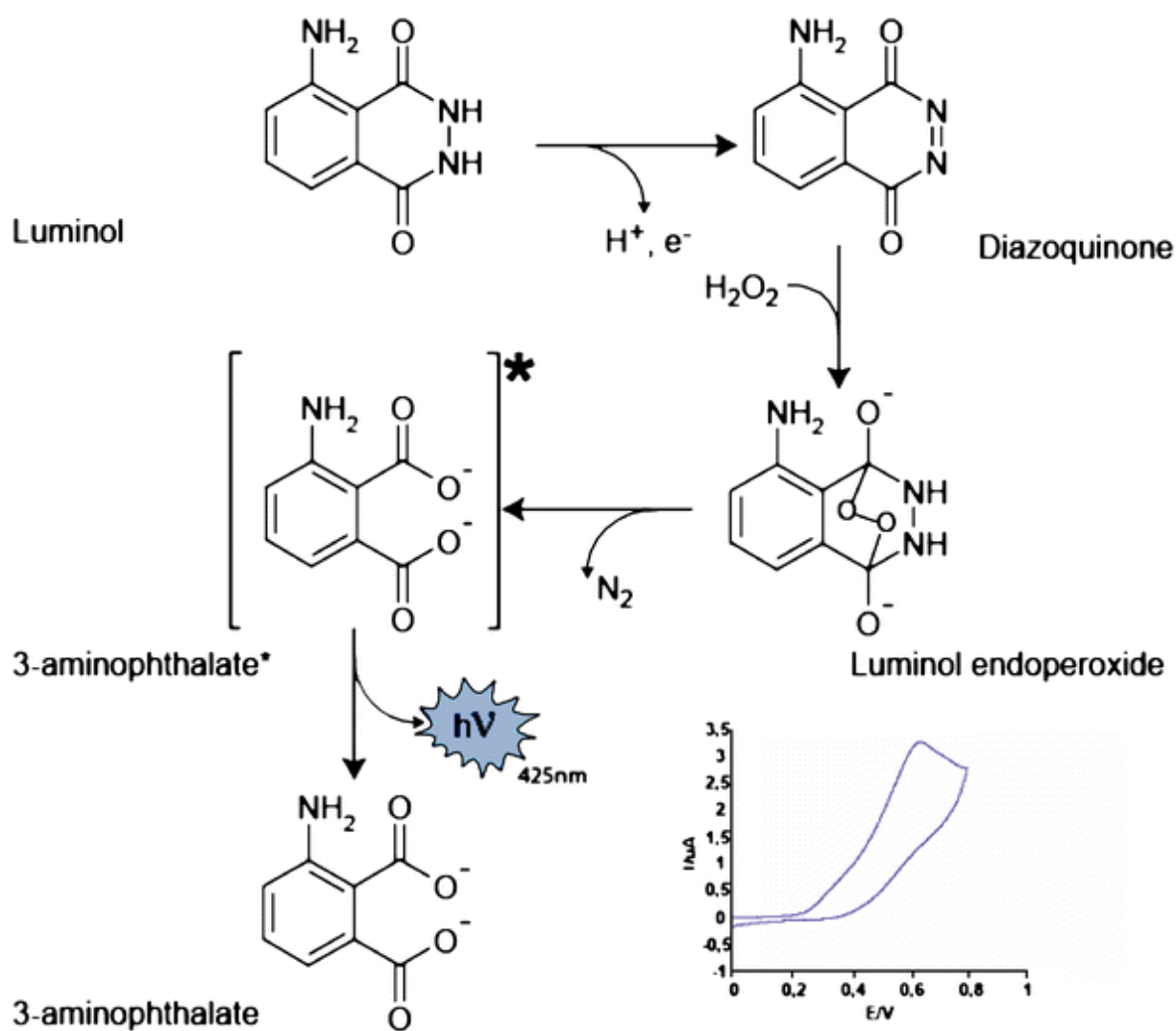


Figure 7. Scheme showing the ECL mechanism of luminol with hydrogen peroxide. Inset: a typical cyclic voltammogram of luminol in aqueous solution. Reproduced from Marquette et al.<sup>42</sup>

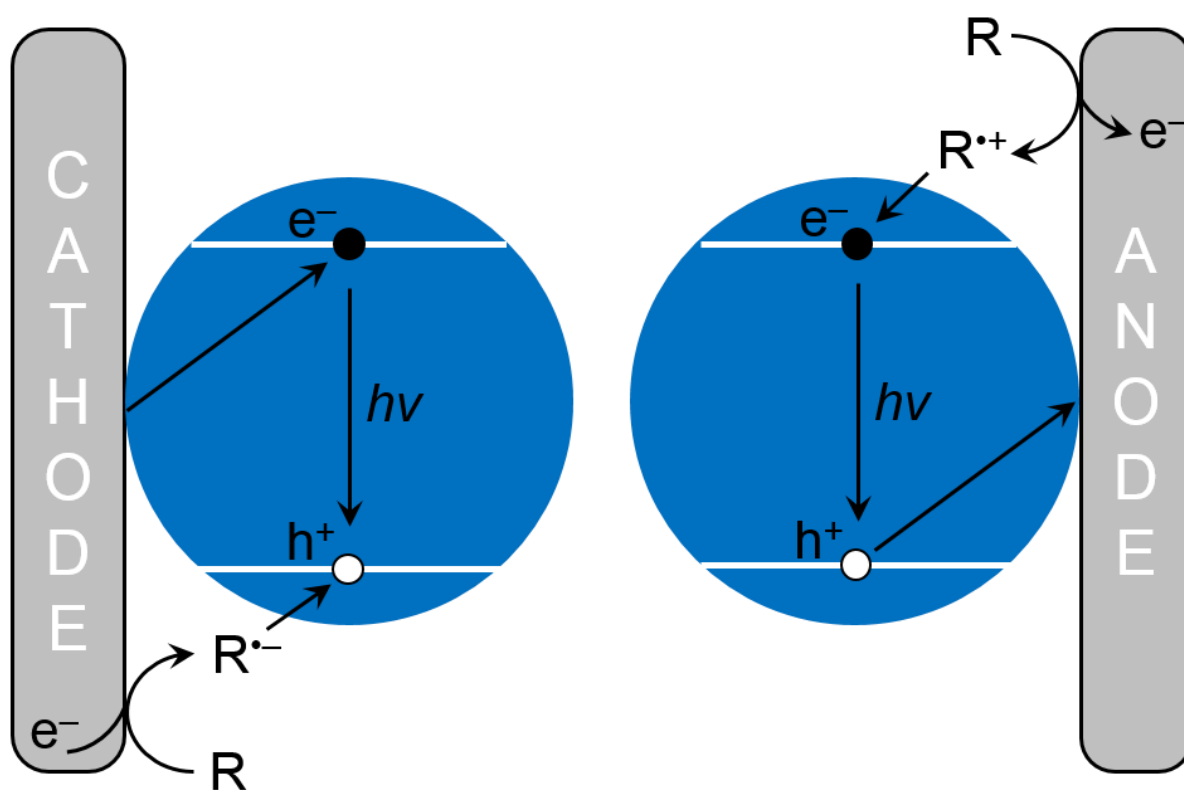


Figure 8. Simplified mechanism of ECL promoted on a nanoparticle or a quantum dot.<sup>52</sup>

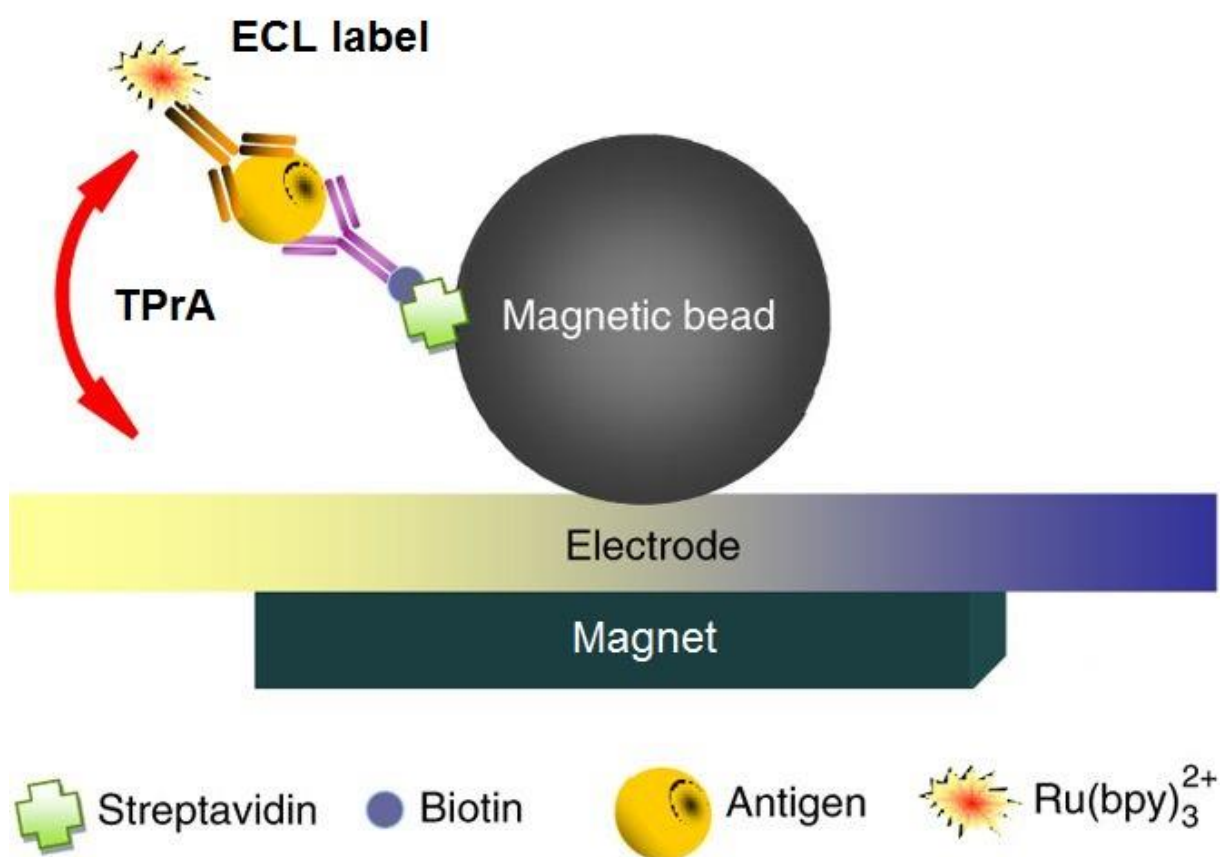


Figure 9. Scheme of a bead-based ECL sandwich immunoassay.<sup>76</sup>